JOSA COMMUNICATIONS

Communications are short papers. Appropriate material for this section includes reports of incidental research results, comments on papers previously published, and short descriptions of theoretical and experimental techniques. Communications are handled much the same as regular papers. Proofs are provided.

Simulation of pulsed squeezing in optical fiber with chromatic dispersion

C. R. Doerr, M. Shirasaki,* and F. I. Khatri

Department of Electrical Engineering and Computer Science and Research, Laboratory of Electronics, Massachusetts Institute of Technology, Cambridge, Massachusetts 02139

Received March 1, 1993; revised manuscript received July 23, 1993

Pulsed squeezing in lossless optical fiber with Kerr nonlinearity and chromatic dispersion is numerically simulated by the use of the linearization approximation. The formalism developed here allows us to predict squeezing for an arbitrary initial complex pulse envelope in a fiber with nonlinearity and dispersion. The results show that squeezing is not necessarily reduced by large temporal and spectral distortions of the pulse caused by dispersion and can even be enhanced in certain cases.

1. INTRODUCTION

The characteristic of a squeezed state is that its quantum uncertainty in one observable is lower than that of a coherent state. This characteristic can permit certain detections to have noise below the standard quantum limit. The most common squeezing is quadrature squeezing in which the observable is one of the quadrature components. Since Slusher *et al.*[1] achieved squeezing in a sodium beam in 1985, many groups have achieved optical squeezing through various methods, such as optical parametric oscillation and amplification[2–4] and four-wave mixing.[5] Both Shelby *et al.*[6] and Levenson *et al.*[7] have accomplished cw squeezing by the use of four-wave mixing in optical fibers. There are also other types of squeezing, such as photon-number squeezing.[8,9]

Quadrature squeezing with a nonlinear interferometer[10] is useful for sub-shot-noise interferometric measurements because it is broadband and, in principle, has no net power loss. Because of the broadband squeezing of the scheme, pulses can be used for squeezing. The main advantage of using pulses instead of cw is that a larger nonlinear phase shift is obtained for a given average power. Pulsed squeezing experiments in fibers have been reported by Bergman and Haus,[11] Rosenbluh and Shelby,[12] and Doerr *et al.*[13]

However, when pulses are used for the squeezing, we encounter a significant concern: pulse envelope distortion that is due to chromatic dispersion. There is only one case in which the pulse envelope propagates undistorted. This is the soliton case, in which the fiber has the appropriate negative dispersion. Analytic theories[14] and computer simulations[15–19] have been developed for this case. Another case that can be analytically solved is the zero-dispersion case. Analytic theories[20] and computer simulations[21] have been developed for this case as well. However, in experiments we cannot always create perfect first-order solitons or have zero dispersion. In addition, often the third-order dispersion must be considered, especially when the pulse is very short. Potasek and Yurke,[22] Drummond and Carter,[16] and Joneckis and Shapiro[23] have investigated squeezing with dispersion in the cw case.

In this Communication we investigate quadrature squeezing by the use of a nonlinear interferometer that uses the Kerr nonlinearity in optical fibers. In particular, this Communication will focus on the squeezing of pulses with dispersion through computer simulation. In Section 2 a method for computing the quantum propagation in an optical fiber with both Kerr nonlinearity and chromatic dispersion is derived. In Section 3 this method is applied to a nonlinear fiber interferometer squeezer and the quantum noise as measured with balanced homodyne detection is calculated. In Section 4 simulation results of squeezing with second-order dispersion for initially unchirped sech-shaped pulses are presented. In Section 5 third-order dispersion is taken into account. Section 6 gives the conclusions.

2. QUANTUM PROPAGATION

To investigate the effects of dispersion on pulsed squeezing, we begin with the quantized nonlinear Schrödinger equation in the Heisenberg picture with self-phase modulation and chromatic dispersion,[10,21,24]

$$\partial\hat{A}/\partial z = i\kappa\hat{A}^{\dagger}\hat{A}\hat{A} + i\mathcal{F}^{-1}\{[\beta(\omega) - \beta_0]\mathcal{F}(\hat{A})\}, \tag{2.1}$$

with $\hat{A}$ as a function of z and t. $\hat{A}$ is the complex envelope of the pulse, κ is the Kerr nonlinear coefficient, t is the time variable, ω is the frequency variable, and z is the propagation distance. $\mathcal{F}$ and $\mathcal{F}^{-1}$ are the Fourier and inverse Fourier transforms, respectively, defined as

$$\mathcal{F}[\hat{A}(t)] \equiv \hat{\tilde{A}}(\omega) \equiv \frac{1}{2\pi}\int_{-\infty}^{\infty} dt\hat{A}(t)\exp(i\omega t), \tag{2.2}$$

$$\mathcal{F}^{-1}[\hat{\tilde{A}}(\omega)] \equiv \hat{A}(t) \equiv \int_{-\infty}^{\infty} d\omega\hat{\tilde{A}}(\omega)\exp(-i\omega t). \tag{2.3}$$

0740-3224/94/010143-07$06.00

$\beta(\omega)$ is the propagation constant of the fiber as a function of frequency, often expanded in a Taylor series about the light carrier frequency ω_0 as[24]

$$\beta(\omega) = \beta_0 + (\omega - \omega_0)\beta_1 + \frac{1}{2}(\omega - \omega_0)^2\beta_2 + \frac{1}{6}(\omega - \omega_0)^3\beta_3 + \ldots, \tag{2.4}$$

where

$$\beta_n = \left(\frac{d^n\beta}{d\omega^n}\right)_{\omega=\omega_0}. \tag{2.5}$$

β_1 represents the group velocity; β_2, the second-order dispersion; β_3, the third-order dispersion, etc. In this paper negative dispersion will refer to $\beta_2 < 0$, that is, the anomalous dispersion/soliton regime.

To obtain an approximate solution to Eq. (2.1), we will make $\hat{A}$ linear. Let

$$\hat{A} = A + \hat{b}, \tag{2.6}$$

where A is a c number representing the classical envelope of the pulse and $\hat{b}$ is the quantum-mechanical part. This approximation is valid for large pump photon numbers and small nonlinear phase shifts and is applicable to most fiber-squeezing experiments. This linearization avoids the singularities that appear when solving the quantum nonlinear Schrödinger equation exactly.[21] Also although the order of the operators in the nonlinear term in Eq. (2.1) has been chosen in a specific way, the dependence on the ordering drops out in the linearization. Ignoring higher-order terms in $\hat{b}$ and canceling the classical terms, we obtain

$$\frac{\partial\hat{b}}{\partial z} = 2i\kappa|A|^2\hat{b} + i\kappa A^2\hat{b}^\dagger + i\mathcal{F}^{-1}\{[\beta(\omega) - \beta_0]\mathcal{F}(\hat{b})\}. \tag{2.7}$$

Next, the pulse is discretized in terms of z and t. Thus $\hat{b}(z,t)$ becomes $\hat{b}_j(n)$ and $A(z,t)$ becomes $A_j(n)$, where the pulse is broken into time intervals of width Δt labeled by integer j and distance intervals of width Δz labeled by integer n. Discretizing Eq. (2.7) and solving for $\hat{b}_j(n+1)$ gives

$$\hat{b}_j(n+1) = [1 + 2i\kappa\Delta z|A_j(n)|^2]\hat{b}_j(n) + i\kappa\Delta z[A_j(n)]^2\hat{b}_j^\dagger(n) + i\Delta z\mathcal{DF}^{-1}\{[\beta(2\pi q/M\Delta t + \omega_0) - \beta_0] \times \mathcal{DF}[\hat{b}_j(n)]\}, \tag{2.8}$$

where $\mathcal{DF}$ and $\mathcal{DF}^{-1}$ are the discrete Fourier and inverse discrete Fourier transforms, respectively, defined as

$$\mathcal{DF}(\hat{b}_j) \equiv \hat{\tilde{b}}_q \equiv \frac{1}{M}\sum_{j=0}^{M-1}\hat{b}_j \exp\left(\frac{i2\pi jq}{M}\right), \tag{2.9}$$

$$\mathcal{DF}^{-1}(\hat{\tilde{b}}_q) \equiv \hat{b}_j \equiv \sum_{q=0}^{M-1}\hat{\tilde{b}}_q \exp\left(\frac{-i2\pi jq}{M}\right). \tag{2.10}$$

M is the number of discrete time points used to represent the pulse. The entire pulse must be included in the region 0 to $M - 1$.

To provide physical insight into the effects of the dispersion, we first consider a simpler case. All the dispersion is neglected except for the second-order dispersion, β_2. The second-order dispersion corresponds to a second derivative in the time domain. Thus Eq. (2.7) becomes

$$\frac{\partial\hat{b}}{\partial z} = 2i\kappa|A|^2\hat{b} + i\kappa A^2\hat{b}^\dagger - \frac{1}{2}i\beta_2\frac{\partial^2\hat{b}}{\partial t^2}, \tag{2.11}$$

and so Eq. (2.8) can be written as

$$\hat{b}_j(n+1) = [1 + 2i\kappa\Delta z|A_j(n)|^2]\hat{b}_j(n) + i\kappa\Delta z[A_j(n)]^2\hat{b}_j^\dagger(n) - \frac{1}{2}i\beta_2\Delta z\frac{\hat{b}_{j-1}(n) - 2\hat{b}_j(n) + \hat{b}_{j+1}(n)}{(\Delta t)^2}. \tag{2.12}$$

From Eq. (2.12), we can see that the dispersion causes coupling of the different time slots in the pulse. At the output the operator at each time slot will be a linear combination of the initial pulse operators, $\hat{b}_j(0)$. Because the quantum-mechanical portion of the initial pulse is in the vacuum state, that portion can be represented by the creation operators, $\hat{a}_j$. Thus we can write

$$\hat{b}_j(n) = \sum_k[\mu_{jk}(n)\hat{a}_k + \nu_{jk}(n)\hat{a}_k^\dagger], \tag{2.13}$$

with

$$[\hat{a}_j, \hat{a}_k^\dagger] = \delta_{jk}, \tag{2.14a}$$

$$[\hat{a}_j, \hat{a}_k] = 0, \tag{2.14b}$$

where $\mu_{jk}(n)$ and $\nu_{jk}(n)$ are the matrix coefficients relating the operators at distance n to the initial operators. Introducing Eq. (2.13) into Eq. (2.12), we find, for the evolution of μ and ν,

$$\mu_{jk}(n+1) = \left[1 + 2i\kappa\Delta z|A_j(n)|^2 + \frac{i\beta_2\Delta z}{(\Delta t)^2}\right]\mu_{jk}(n) + i\kappa\Delta z[A_j(n)]^2\nu_{jk}^*(n) - \frac{i\beta_2\Delta z}{2(\Delta t)^2}[\mu_{j-1,k}(n) + \mu_{j+1,k}(n)], \tag{2.15}$$

$$\nu_{jk}(n+1) = \left[1 + 2i\kappa\Delta z|A_j(n)|^2 + \frac{i\beta_2\Delta z}{(\Delta t)^2}\right]\nu_{jk}(n) + i\kappa\Delta z[A_j(n)]^2\mu_{jk}^*(n) - \frac{i\beta_2\Delta z}{2(\Delta t)^2}[\nu_{j-1,k}(n) + \nu_{j+1,k}(n)]. \tag{2.16}$$

The initial conditions for these evolution equations are

$$\mu_{jk}(0) = \delta_{jk}, \tag{2.17}$$

$$\nu_{jk}(0) = 0. \tag{2.18}$$

Thus to calculate the quantum propagation at each Δz step the classical pulse envelope evolution is calculated by the use of the classical nonlinear Schrödinger equation [Eq. (2.1) with $\hat{A}$ as a c number] through standard fiber pulse propagation algorithms,[24] and the μ and ν evolutions are calculated by the use of Eqs. (2.15) and (2.16). However, because of the rough approximation of the second derivative in Eq. (2.12), the simulation must use small step sizes to obtain good numerical accuracy. A numerically more robust approach, plus one that permits the inclusion of higher-order dispersion, is obtained by returning to Eq. (2.8).

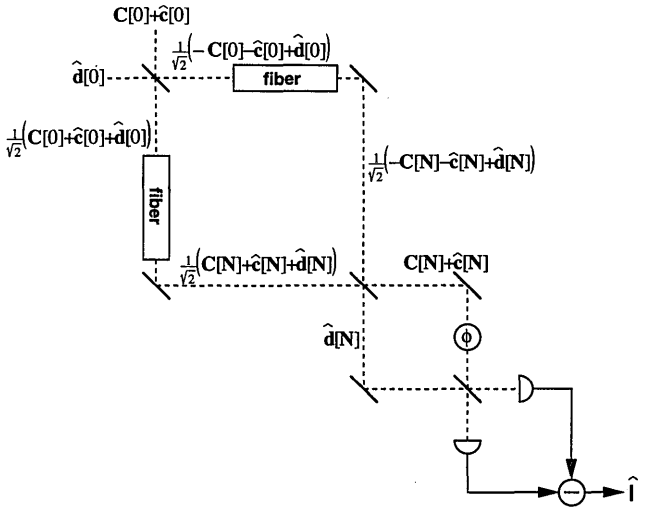

Fig. 1. Squeezing schematic consisting of a fiber nonlinear interferometer and a balanced homodyne detector.

First, we can easily show from Eq. (2.13) that

$$\hat{\tilde{b}}_q(n) = \sum_k [\tilde{\mu}_{qk}(n)\hat{a}_k + \tilde{\nu}_{qk}(n)\hat{a}_k^\dagger], \tag{2.19}$$

where $\tilde{\mu}_{qk}$ and $\tilde{\nu}_{qk}$ are the discrete Fourier transforms of the columns of μ_{jk} and ν_{jk}.

Thus, substituting Eqs. (2.13) and (2.19) into Eq. (2.8), we find for the evolution of μ and ν that

$$\begin{aligned}\mu_{jk}(n+1) = {} & [1 + 2i\kappa\Delta z|A_j(n)|^2]\mu_{jk}(n) \\ & + i\kappa\Delta z[A_j(n)]^2\nu_{jk}^*(n) \\ & + i\Delta z\mathcal{D}\mathcal{F}^{-1}\{[\beta(2\pi q/M\Delta t + \omega_0) - \beta_0]\tilde{\mu}_{qk}(n)\},\end{aligned} \tag{2.20}$$

$$\begin{aligned}\nu_{jk}(n+1) = {} & [1 + 2i\kappa\Delta z|A_j(n)|^2]\nu_{jk}(n) \\ & + i\kappa\Delta z[A_j(n)]^2\mu_{jk}^*(n) \\ & + i\Delta z\mathcal{D}\mathcal{F}^{-1}\{[\beta(2\pi q/M\Delta t + \omega_0) - \beta_0]\tilde{\nu}_{qk}(n)\}.\end{aligned} \tag{2.21}$$

In essence, the last terms in Eqs. (2.20) and (2.21) mean that we take the Fourier transform of the columns of μ [or ν in the case of Eq. (2.21)], multiply each column by $\beta(2\pi q/M\Delta t + \omega_0) - \beta_0$, and then take the inverse Fourier transform of each column. The initial conditions are the same as given by Eqs. (2.17) and (2.18).

All the results of this paper were calculated by the use of Eqs. (2.20) and (2.21) because the results given by these equations, although the same as those given by Eqs. (2.15) and (2.16) when only nonlinearity and second-order dispersion was considered, were numerically more stable. The propagation technique given by Eqs. (2.20) and (2.21) is similar to the split-step Fourier method, a method commonly used in nonlinear propagation simulations.[17,18,24]

3. SQUEEZING SCHEME AND NOISE CALCULATION

In Section 2 the propagation of the classical and quantum-mechanical parts of a pulse through a lossless fiber of length $N\Delta z$ with Kerr nonlinearity and dispersion was calculated, with the initial state $A(0) + \hat{b}(0)$ and the final state $A(N) + \hat{b}(N)$. Here, this calculation is applied to determine the noise level created by the nonlinear fiber interferometer squeezer shown in Fig. 1. The pump, $\hat{C}(0)$, enters one port of the nonlinear interferometer, and vacuum fluctuations, $\hat{d}(0)$, enter the other port. If we follow the linearization approximation, the pump can be separated into its classical and quantum-mechanical parts, $C(0)$ and $\hat{c}(0)$, respectively. The classical part of the vacuum, $\hat{d}(0)$, is zero. $\hat{c}$ and $\hat{d}$ are in the vacuum state.

This light enters the interferometer and is split by the first beam splitter. Let A_L and $\hat{b}_L$ represent the classical and quantum-mechanical parts of the light in the left arm of the interferometer, and let A_R and $\hat{b}_R$ represent those for the right arm. Thus,

$$A_L(0) = \frac{1}{(2)^{1/2}}C(0), \tag{3.1}$$

$$\hat{b}_L(0) = \frac{1}{(2)^{1/2}}[\hat{c}(0) + \hat{d}(0)], \tag{3.2}$$

$$A_R(0) = -\frac{1}{(2)^{1/2}}C(0), \tag{3.3}$$

$$\hat{b}_R(0) = \frac{1}{(2)^{1/2}}[-\hat{c}(0) + \hat{d}(0)]. \tag{3.4}$$

A and $\hat{b}$ can be evolved by the use of the results of Section 2. Because of the linearization approximation, the evolution is linear in $\hat{b}$. This implies that the evolutions of $\hat{c}$ and $\hat{d}$ can be considered independently and that

$$\hat{b}_L(N) = \frac{1}{(2)^{1/2}}[\hat{c}(N) + \hat{d}(N)], \tag{3.5}$$

$$\hat{b}_R(N) = \frac{1}{(2)^{1/2}}[-\hat{c}(N) + \hat{d}(N)]. \tag{3.6}$$

Exiting the interferometer are $C(N) + \hat{c}(N)$ and $\hat{d}(N)$. The pump, $C(N) + \hat{c}(N)$, is phase shifted by ϕ, and then the signals are homodyne detected. In the resulting detector current, $\hat{I}$, the quantum-mechanical part of the pump, $\hat{c}(N)$, will appear in only higher-order terms and so can be neglected.

Assuming that the detectors measure the light intensity with perfect efficiency, we can show that the balanced detector current is[10]

$$\hat{I}_j = C_j^*(N)\exp(-i\phi)\hat{d}_j(N) + C_j(N)\exp(i\phi)\hat{d}_j^\dagger(N). \tag{3.7}$$

From now on, we shall suppress the argument N.

We can see from Eqs. (2.20) and (2.21) that the evolutions of μ and ν are independent of the sign of the pump, A, and so are the same for both arms of the interferometer. Combining Eqs. (2.13), (3.5), and (3.6) with Eq. (3.7), we get

$$\begin{aligned}\hat{I}_j = {} & \frac{1}{(2)^{1/2}}C_j^*\exp(-i\phi) \\ & \times \sum_k [\mu_{jk}(\hat{a}_{kL} + \hat{a}_{kR}) + \nu_{jk}(\hat{a}_{kL}^\dagger + \hat{a}_{kR}^\dagger)] \\ & + \frac{1}{(2)^{1/2}}C_j\exp(i\phi) \\ & \times \sum_k [\mu_{jk}^*(\hat{a}_{kL}^\dagger + \hat{a}_{kR}^\dagger) + \nu_{jk}^*(\hat{a}_{kL} + \hat{a}_{kR})],\end{aligned} \tag{3.8}$$

where $\hat{a}_L$ and $\hat{a}_R$ are the annihilation operators representing the initial states of $\hat{b}_L$ and $\hat{b}_R$; $\hat{a}_L$ and $\hat{a}_R$ commute, which is easily shown from Eqs. (3.2) and (3.4) and the fact that $\hat{c}$ and $\hat{d}$ commute.

The power spectrum of the current at zero frequency (frequency low compared with the width of the pulse spectrum), Φ_0, is given by[10]

$$\Phi_0 \equiv |\hat{I}_0|^2 = \frac{1}{2M^2} \sum_{jl} \langle \hat{I}_l I_{l-j} + \hat{I}_{l-j} \hat{I}_l \rangle. \tag{3.9}$$

The squeezing ratio, R, defined as the noise normalized to shot noise, is[10]

$$R = \frac{\Phi_0|_{(\mu,\nu)}}{\Phi_0|_{(\mu_{jk}=\delta_{jk},\nu_{jk}=0)}}. \tag{3.10}$$

Using the facts that

$$\langle \hat{a}_j \hat{a}_k^\dagger \rangle = \delta_{jk}, \tag{3.11}$$

$$\langle \hat{a}_j \hat{a}_k \rangle = \langle \hat{a}_j^\dagger \hat{a}_k \rangle = \langle \hat{a}_j^\dagger \hat{a}_k^\dagger \rangle = 0, \tag{3.12}$$

we find, after some algebra, that

$$R = \frac{\sum_{jkl} \mathrm{Re}[C_l^* C_j^* \exp(-2i\phi)(\mu_{lk}\nu_{jk} + \mu_{jk}\nu_{lk}) + C_l C_j^* (\mu_{lk}^* \mu_{jk} + \nu_{lk}^* \nu_{jk})]}{\sum_l |C_l|^2}. \tag{3.13}$$

The maximum (minimum) squeezing ratio, obtained by appropriately adjusting the local oscillator phase, ϕ, is

$$R_{\max(\min)} = \frac{\sum_{jkl} \{\mathrm{Re}[C_l C_j^* (\mu_{lk}^* \mu_{jk} + \nu_{lk}^* \nu_{jk})] \pm |C_l^* C_j^* (\mu_{lk}\nu_{jk} + \mu_{jk}\nu_{lk})|\}}{\sum_l |C_l|^2}. \tag{3.14}$$

The squeezing is calculated as follows. Start with a pump with its time-discretized pulse envelope defined by C, μ as the identity matrix, and ν as a matrix of zeros (to start the vacuum in a coherent state). Then propagate C by the use of the classical nonlinear Schrödinger equation, and at each propagation step calculate the new μ and ν matrices by the use of Eqs. (2.20) and (2.21) with $A = 1/(2)^{1/2}C$. At the end of the propagation, the amounts of squeezing, $R_{\min}$, and antisqueezing, $R_{\max}$, are calculated from Eq. (3.14). A good way to check the simulation is that R should equal 1 when $\phi = 0$.

4. RESULTS WITH SECOND-ORDER DISPERSION

To test the simulation, the results for the soliton and dispersionless cases were shown to agree with the existing analytic theories for these cases.[10,14] Also, when the nonlinearity was set to zero, the results gave shot noise ($R = 1$), regardless of the dispersion, as expected. In addition, shot noise was always obtained when $\phi = 0$.

Figure 2 shows the amounts of squeezing and antisqueezing versus second-order dispersion. The initial pulse in each arm of the interferometer was an unchirped sech-shaped amplitude pulse with an intensity FWHM of 200 fs. The nonlinearity was $\kappa = 1.5\ \mathrm{W}^{-1}\ \mathrm{km}^{-1}$, and the peak intensity was 1037 W. This result corresponds to a soliton when $\beta_2 = -20\ \mathrm{ps}^2/\mathrm{km}$ with a soliton period of 1.0 m. The pulse was propagated for distances of 0.64, 1.28, 1.92, and 2.56 m, corresponding to nonlinear phase shifts in the soliton cases of 0.5, 1.0, 1.5, and 2.0 rad, respectively.

One interesting result is that until high phase shifts are used, the soliton squeezing is not much better than the zero-dispersion squeezing. There are two primary reasons for this. The first is that in the soliton case the local oscillator is a sech-shaped pulse, which is not the optimum local oscillator for a soliton (the actual optimum local oscillator is a linear combination of the soliton photon number and phase perturbation functions).[14,25] The second is that in the soliton case the entire pulse experiences a nonlinear phase shift of $0.5\kappa|A_{\mathrm{peak}}|^2 z$ (A_{peak} is the peak amplitude of the pulse, z is the distance traveled), whereas in the dispersionless case, for the same initial pulse, the peak of the pulse experiences a larger nonlinear phase shift of $\kappa|A_{\mathrm{peak}}|^2 z$. The wings of the pulse in the dispersionless case experience less nonlinear phase shift, though, ultimately leaving the soliton with the highest total squeezing.

Another interesting result is that the squeezing is actually increased in the low positive dispersion regime. This can be understood by looking at the pulse shape for $\beta_2 = +5\ \mathrm{ps}^2/\mathrm{km}$ in Fig. 3, which shows the pulse after it propagates 2.56 m for different values of β_2. A pulse undergoing nonlinearity and positive dispersion tends to steepen its sides and become more like a square pulse.[24] This makes the squeezing more uniform across the pulse, increasing the amount of squeezing.

In the low negative dispersion regime, the pulse becomes a higher-order soliton. Despite the increase in peak power, the squeezing decreases, probably because of the large wings that form (see the case for $\beta_2 = -1\ \mathrm{ps}^2/\mathrm{km}$ in Fig. 3). These wings have low peak power and so are not highly squeezed.

5. INCLUSION OF THIRD-ORDER DISPERSION

Figure 4 shows the same case as in Fig. 2 but with the addition of third-order dispersion ($\beta_3 = +0.1\ \mathrm{ps}^3/\mathrm{km}$, a typical value for third-order dispersion in fiber). At higher phase shifts, the third-order dispersion reduces the squeezing at zero and very small positive β_2. However, for small negative β_2, the third-order dispersion lessens the reduction of the squeezing by the second-order

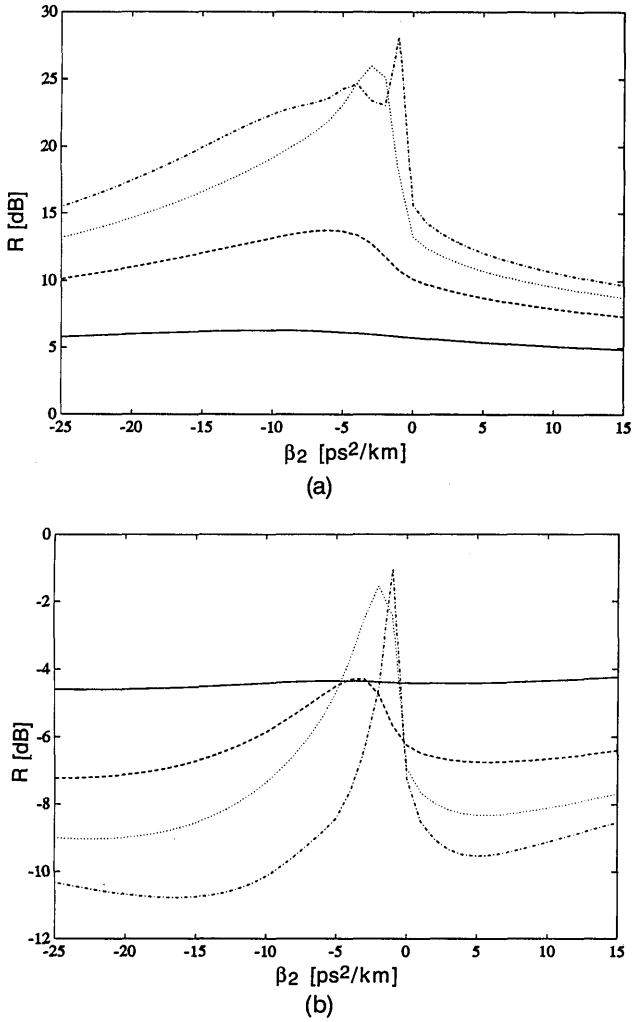

Fig. 2. (a) Antisqueezing and (b) squeezing versus second-order dispersion. The input pulse is a 200-fs sech that is a soliton at $\beta_2 = -20$ ps^2/km. The solid curve is for $l = 0.64$ m, the dashed curve is for $l = 1.28$ m, the dotted curve is for $l = 1.92$ m, and the dashed–dotted curve is for $l = 2.56$ m. These lengths correspond to nonlinear phase shifts for the soliton of 0.5, 1.0, 1.5, and 2.0 rad, respectively.

dispersion. This can be partially understood by comparing the pulse shape for $\beta_2 = -1$ ps^2/km in Fig. 3 and the pulse shape in Fig. 5. As we can see, the third-order dispersion suppresses the formation of large wings on the pulse. We found that the third-order dispersion effect is negligible for $|\beta_2| > 10$ ps^2/km, and so for the case of Fig. 4 it has no noticeable effect on the soliton squeezing. In addition, the third-order dispersion effect quickly becomes negligible for longer pulses (>1 ps) because of the small spectral bandwidth across which β_2 can be considered constant.

Figure 6 shows the same case as in Fig. 2, except the initial pulse now has an intensity FWHM of 100 fs. This pulse is a first-order soliton at $\beta_2 = -5$ ps^2/km with a soliton period of 1.0 m. This case is used to represent the situation in which we have a very short pulse yet not enough peak power to have a soliton at the traditional $\beta_2 = -20$ ps^2/km. In this case the squeezing is actually enhanced at $\beta_2 = 0$ by the third-order dispersion despite the fact that the spectrum is distorted with large phase shifts. Also, the reduction of the squeezing by low nega-

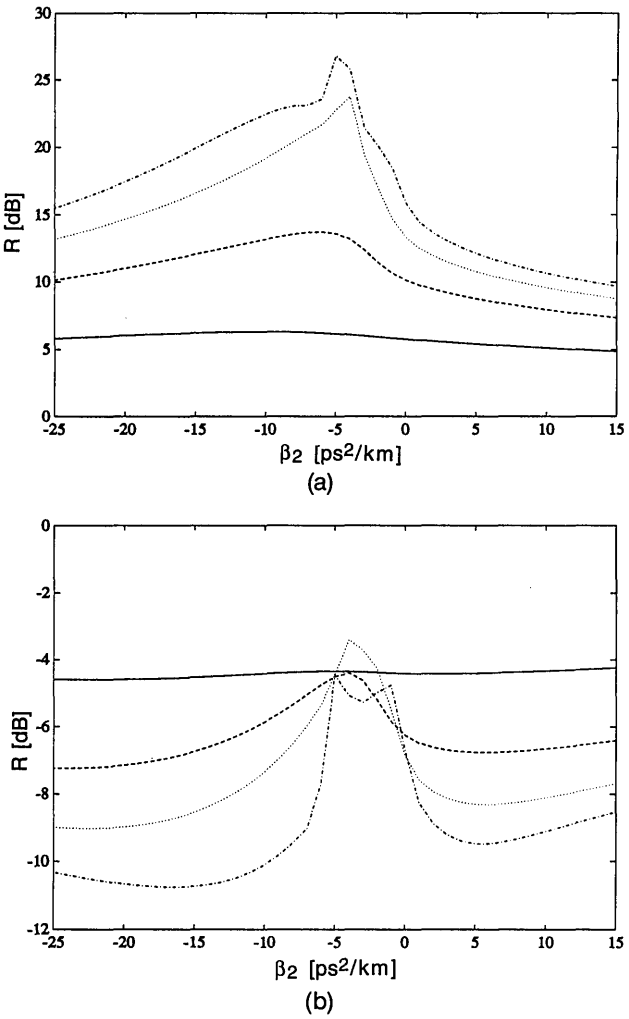

Fig. 4. (a) Antisqueezing and (b) squeezing versus second-order dispersion with third-order dispersion included ($\beta_3 = 0.1$ ps^3/km). All other parameters are the same as in Fig. 2.

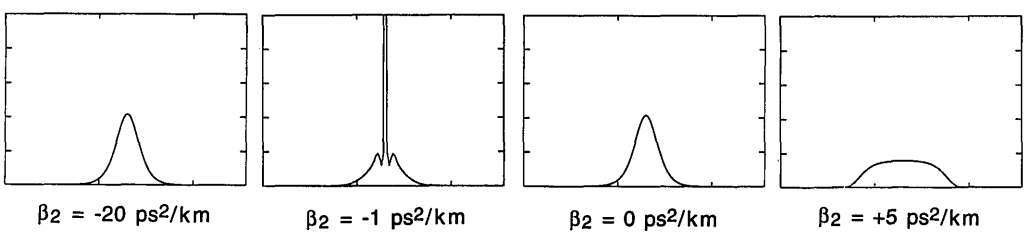

Fig. 3. Pulse shapes at the output after traveling $l = 2.56$ m with various amounts of second-order dispersion. Parameters are the same as in Fig. 2. The coordinates are intensity versus time, and all pulses have the same scale.

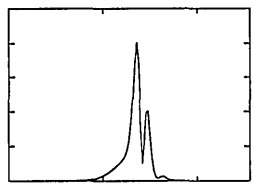

Fig. 5. Pulse shape at the output after traveling $l = 2.56$ m with $\beta_2 = -1$ ps^2/km and $\beta_3 = 0.1$ ps^3/km. Parameters are the same as in Fig. 4. The coordinates are intensity versus time with the same scale as in Fig. 3.

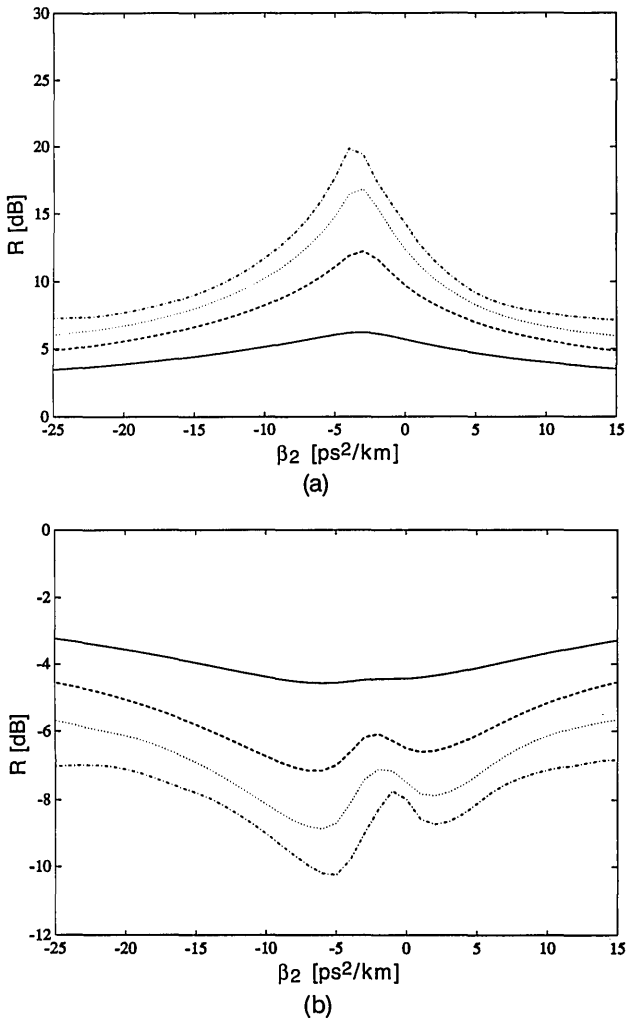

Fig. 6. (a) Antisqueezing and (b) squeezing versus second-order dispersion with third-order dispersion included ($\beta_3 = 0.1$ ps^3/km). The input pulse is a sech as in Figs. 2–5, except the pulse intensity FWHM is 100 fs. All other parameters are the same.

tive β_2 is small, probably because the third-order dispersion dominates in the higher-order soliton regime in this case, and large wings are not developed.

6. CONCLUSIONS

The effects of chromatic dispersion on pulsed squeezing in fibers were numerically investigated. It was found that temporal pulse distortions created by dispersion do not necessarily cause the squeezing to deteriorate. For an initially unchirped sech-shaped pulse, the best squeezing was obtained in the first-order soliton regime, and the next best squeezing was obtained in the small normal dispersion regime. It was found that in the low anomalous dispersion regime, where the pulse becomes a higher-order soliton, the squeezing is reduced. Third-order dispersion can either reduce or enhance the squeezing depending on the pulse width and the second-order dispersion. The third-order dispersion lessens the squeezing deterioration due to small anomalous dispersion, and it has no significant effect at large values of second-order dispersion ($|\beta_2| > 10$ ps^2/km, approximately).

Our results offer suggestions for future research. We found that we do not need a perfect soliton or exact zero dispersion to achieve reasonable squeezing. If one is squeezing near zero dispersion, though, one should keep the pulse spectrum on the normal side of the dispersion in order to avoid higher-order soliton effects. In fact, normal dispersion squeezing could be useful. Normal dispersion squeezing was found to be higher than the dispersionless squeezing; the average pulse peak power in normal dispersion squeezing is lower, reducing the antisqueezing and thus also the squeezing level sensitivity to the local oscillator phase; because dispersion-shifted fibers often have a smaller mode field diameter, we could use a shorter fiber for the squeezing and we could use light with wavelengths below 1.3 μm, where it is difficult to make fiber with anomalous dispersion.

Finally, our simulation results show that, at least so far as pulse distortions caused by dispersion are concerned, squeezing is not so fragile as one might expect.

ACKNOWLEDGMENTS

We thank H. A. Haus and F. X. Kärtner for useful discussions and J. L. Pan and J. C. Chen for their help with the computer. This research was sponsored by the Charles Stark Draper Laboratory and by Fujitsu Laboratories Ltd., Japan. Also, portions of this research were conducted by the use of the resources of the Cornell Theory Center, which receives major funding from the National Science Foundation and IBM Corporation, with additional support from New York State Science and Technology Foundation and members of the Corporate Research Institute.

*M. Shirasaki is also with Fujitsu Laboratories Ltd., Kawasaki, Japan.

REFERENCES

1. R. E. Slusher, L. W. Hollberg, B. Yurke, J. C. Mertz, and J. F. Valley, "Observation of squeezed states generated by four-wave mixing in an optical cavity," Phys. Rev. Lett. **55,** 2409 (1985).
2. L.-A. Wu, M. Xiao, and H. J. Kimble, "Squeezed states of light from an optical parametric oscillator," J. Opt. Soc. Am. B **4,** 1465 (1987).
3. R. E. Slusher, P. Grangier, A. LaPorta, B. Yurke, and M. J. Potasek, "Pulsed squeezed light," Phys. Rev. Lett. **59,** 2566 (1987).
4. O. Aytür and P. Kumar, "Pulsed twin beams of light," Phys. Rev. Lett. **65,** 1551 (1990).
5. H. P. Yuen and J. H. Shapiro, "Generation and detection of two-photon coherent states in degenerate four-wave mixing," Opt. Lett. **4,** 334 (1979).

6. R. M. Shelby, M. D. Levenson, S. H. Perlmutter, R. G. DeVoe, and D. F. Walls, "Broadband parametric deamplification of quantum noise in an optical fiber," Phys. Rev. Lett. **57,** 691 (1986).
7. M. D. Levenson, R. M. Shelby, M. Reid, and D. F. Walls, "Quantum nondemolition detection of optical quadrature amplitudes," Phys. Rev. Lett. **57,** 2473 (1986).
8. M. Kitagawa and Y. Yamamoto, "Number-phase minimum-uncertainty state with reduced number uncertainty in a Kerr nonlinear interferometer," Phys. Rev. A **34,** 3974 (1986).
9. S. Machida, Y. Yamamoto, and Y. Itaya, "Observation of amplitude squeezing in a constant-current-driven semiconductor laser," Phys. Rev. Lett. **58,** 1000 (1987).
10. M. Shirasaki and H. A. Haus, "Squeezing of pulses in a nonlinear interferometer," J. Opt. Soc. Am. B **7,** 30 (1990).
11. K. Bergman and H. A. Haus, "Squeezing in fibers with optical pulses," Opt. Lett. **16,** 663 (1991).
12. M. Rosenbluh and R. M. Shelby, "Squeezed optical solitons," Phys. Rev. Lett. **66,** 153 (1991).
13. C. R. Doerr, I. Lyubomirsky, G. Lenz, J. Paye, H. A. Haus, and M. Shirasaki, "Optical squeezing with a short fiber," in *Quantum Electronics and Laser Science Conference*, Vol. 12 of 1993 OSA Technical Digest Series (Optical Society of America, Washington, D.C., 1993), paper QFF-3.
14. H. A. Haus and Y. Lai, "Quantum theory of soliton squeezing: a linearized approach," J. Opt. Soc. Am. B **7,** 386 (1990).
15. S. J. Carter, P. D. Drummond, M. D. Reid, and R. M. Shelby, "Squeezing of quantum solitons," Phys. Rev. Lett. **58,** 1841 (1987).
16. P. D. Drummond and S. J. Carter, "Quantum-field theory of squeezing in solitons," J. Opt. Soc. Am. B **4,** 1565 (1987).
17. P. D. Drummond, S. J. Carter, and R. M. Shelby, "Time dependence of quantum fluctuations in solitons," Opt. Lett. **14,** 373 (1989).
18. R. M. Shelby, P. D. Drummond, and S. J. Carter, "Phase-noise scaling in quantum soliton propagation," Phys. Rev. A **42,** 2966 (1990).
19. F. Singer, M. J. Potasek, J. M. Fang, and M. C. Teich, "Femtosecond solitons in nonlinear optical fibers: classical and quantum effects," Phys. Rev. A **46,** 4192 (1992).
20. M. Shirasaki, "Quantum-noise reduction in a phase-sensitive interferometer using nonclassical light produced through Kerr media," Opt. Lett. **16,** 171 (1991).
21. K. J. Blow, R. Loudon, and S. J. D. Phoenix, "Exact solution for quantum self-phase modulation," J. Opt. Soc. Am. B **8,** 1750 (1991).
22. M. J. Potasek and B. Yurke, "Squeezed-light generation in a medium governed by the nonlinear Schrödinger equation," Phys. Rev. A **35,** 3974 (1987).
23. L. G. Joneckis and J. H. Shapiro, "Quantum propagation in single-mode fiber," in *Quantum Electronics and Laser Science Conference*, Vol. 12 of 1993 OSA Technical Digest Series (Optical Society of America, Washington, D.C., 1993), paper QFF-4.
24. G. P. Agarwal, *Nonlinear Fiber Optics* (Academic, New York, 1989).
25. Y. Lai, "Quantum theory of optical solitons," Ph.D. dissertation (Massachusetts Institute of Technology, Cambridge, Mass., 1989).